ICC 2021 - IEEE International Conference on Communications | 978-1-7281-7122-7/21/$31.00 ©2021 IEEE | DOI: 10.1109/ICC42927.2021.9500856

Optimum Routing and Slot Formatting in UAV-Assisted 5G Networks

Ahmed Elbery*, Hossam S. Hassanein*, Hatem Abouzeid†, and Akram Bin Sediq† Gary Boudreau†
*School of Computing, Queen's University, Kingston, Ontario, Canada
†Ericsson, Ottawa, Canada
E-mails:{aelbery@vt.edu, hossam@cs.queensu.ca, hatem.abou-zeid@ericsson.com,
akram.bin.sediq@ericsson.com, gary.boudreau@ericsson.com}

***Abstract*—Unmanned Aerial Vehicles (UAV) are expected to play a crucial role in the future of 5G and beyond. However, designing efficient routing protocols for UAV is challenging due to the mobility and energy constraints. This problem becomes harder in UAV-assisted 5G networks because of its impact on the time slot assignment for the uplink and downlink in Time Division Duplex (TDD) frame structure. Thus, in this paper, we propose a new optimum routing technique for UAV-assisted TTD 5G networks, the Optimized Load-Balancing Routing (OLBR). The optimum routing problem is formulated in such a way that the decision variables are used to compute the time slot assignment in the 5G connection between UAV nodes. The objective of the optimization model is to minimize the network-wide delay. By distributing traffic across different alternative routes, OLBR minimizes network congestion, resulting in shorter queuing delays. Such a load-balancing also decreases the possibility of node failure due to energy depletion. The proposed OLBR is compared to the shortest path routing using Monte Carlo simulation on two different network topologies at different network traffic loads. The simulation results show that the OLBR produces significant savings in network-wide packet delay compared to the shortest path.**

***Index Terms*—UAV Routing Protocols, UAV Assisted 5G, Load-Balancing, System-Optimum Routing.**

I. Introduction

Enabled by the rapid deployment of low-cost radio interfaces, Global Positioning System (GPS), sensors, and embedded microcomputers, Unmanned Aerial Vehicles (UAVs) have garnered significant interest from researchers in the areas of disaster relief operations [1], emergency communication [2], surveillance and reconnaissance [3], autonomous tracking [4], managing wildfire [5], remote sensing [6], and traffic monitoring and surveillance [7]. Many of these applications depend on a fleet of UAVs to cooperatively achieve a certain task. Such cooperation between UAVs creates a new type of Ad-hoc networks, the Flying Ad-hoc Networks (FANETs) [8].

In the Fifth Generation (5G) cellular networks, UAVs are expected to replace the ground Base Stations (BSs) in many cases. This is attributed to the easy and fast deployment of UAVs. For instance, using UAVs is an efficient alternative to using BSs in certain situations such as outdoor music festivals, sporting events, or emergencies [1], [2]. The importance of UAVs becomes prominent in the areas where installing BSs is difficult due to space limitations or administrative barriers. As a proof of concept, in 2016, Nokia deployed a quadcopter drone equipped with a 2 kg weight 4G mobile base station to provide coverage over a remote area in Scotland [9].

Using UAVs to enhance the 5G coverage introduces the multi-hop connectivity and the required packet routing techniques to the 5G networks. Due to the unique characteristics of UAVs, designing efficient routing protocols for FANETs is a challenging task. The high mobility and dynamic nature of UAV networks possess a major challenge. The routing protocols should be able to deal with this mobility and compute alternative routes quickly and efficiently.

An important aspect of the routing in the 5G New Radio (NR) is its relationship to the physical layer time slot formats. In 5G NR, downlink and uplink transmissions are organized into a 10 ms frames [10]. Each frame is divided into 10 subframes, $1ms$ each. Based on the numerology (μ), each subframe is divided into 2^{μ} time slots, $\frac{1}{2^{\mu}}\,ms$ each. In each time slot, there are 14 OFDM symbols [10]. Figure 1 shows the frame structure for subcarrier spacing configuration $\mu = 3$.

As described in [11], each OFDM symbol can be assigned to either Uplink (U), Downlink (D), or to be a Flexible one (F) that can be used for both transmission directions. This assignment determines the Slot Format (SF), which is identified by SF Index (SFI) in [11]. Although these specifications are for the User Equipment (UE), they can be applied to the links between UAV base stations in the Integrated Access and Backhauling (IAB) [12]. In such an environment, selecting the suitable SFI for a connection between two UAV nodes depends on the traffic load between them, which is

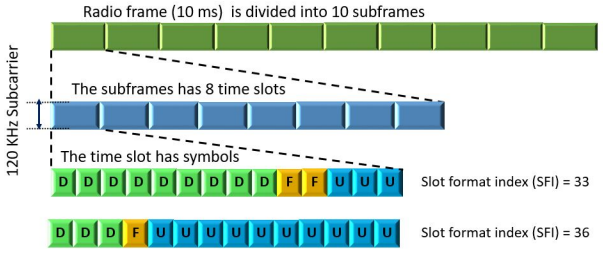

Figure 1. The 5G radio frame structure for $\mu = 3$ with 2 SFI examples.

This research is supported by a grant from the Natural Sciences and Engineering Research Council of Canada (NSERC) under grant number STPGP 521432-2018

978-1-7281-7122-7/21/$31.00 ©2021 IEEE

Authorized licensed use limited to: Queen's University. Downloaded on December 01,2021 at 20:31:36 UTC from IEEE Xplore. Restrictions apply.

controlled by the routing technique. So, routing and link physical configuration should be jointly optimized to achieve the best network performance.

Thus, contributions of this paper are:

- We propose a novel routing technique for UAV-assisted 5G networks, the Optimized Load-Balance Routing (OLBR), that minimizes the network-wide packet delay by utilizing traffic load-balancing. The OLBR can be utilized as a link-state routing optimization technique [13].
- The optimization problem is formulated in a novel way that the uplink and downlink physical capacities can be jointly optimized by solving this optimization problem iteratively.
- The non-linear optimization problem is converted into a linear problem based on the convexity of its objective function.
- The proposed model is compared to the shortest path routing, which is the base for most routing techniques. To address the traffic demand uncertainties, Monte Carlo simulation is used for comparison between the OLBR and shortest path based routing on two different network topologies at different traffic rates

The proposed OLBR model can be used for ground base stations without UAVs. However, the network size is expected to be large, and the problem will be intractable. In UAV-assisted 5G coverage, the OLBR utilized the fact that the number of UAV nodes is relatively small, and these nodes have at least one connection to ground base stations as shown in Fig. 2. In such architecture, the UAV network represents an autonomous system that can be separately optimized. Based on these facts, the complexity of the optimization model can be overcome, where the problem will be small. Moreover, complex problems can be solved by a ground base station which has more computational power and unlimited energy source.

The main idea behind the proposed technique is to load-balance the traffic across different alternative routes in such a way that minimizes the network-wide delay. The average packet delay is computed based on the M/M/1/K model [14], which produces a non-linear optimization problem. Then, based on the problem characteristics, we transformed it into a linear problem that can be solved in polynomial time. The OLBR uses the flow label provided in IPv6 [15], which makes routing faster. More importantly, the OLBR optimization does not need to be solved by every individual node. The reason is that the formulated linear program is a system-optimum model, which has a universal solution that can be used by all nodes. So, it can be solved by a BS, and the solution (which is a vector of real values) can be broadcasted to all the UAVs in the fleet. Then, each UAV can use the solution parameters associated with its interfaces to route packets. This way, the routing computation is minimized on the UAV-nodes, which have limited energy. To the best of our knowledge, this is the first work that jointly optimizes traffic routing and TDD slot formats of the IAB physical connections in 5G NR.

The remainder of the paper is organized as follows. In Section II, the proposed model is presented. Then, the simulation setup and results are introduced in Section III before the conclusion in Section IV.

II. The Proposed Routing Algorithm

This section describes the proposed routing algorithm. We, firstly, describe the network model is in Subsection II-A, then node model will be explained in Subsection II-B. Afterward, the routing optimization problem is presented.

A. Network Model and Mathematical Representation

In our model, the network has a set of UAV nodes, as shown in Fig. 2. Some of these UAV nodes receive data from ground stations (such as users or BSs) while others generate their own traffic (i.e., mission-oriented traffic such as video surveillance UAVs). We consider all these nodes (either those generating traffic or receiving traffic from ground stations) as traffic sources.

In our model, each communication link is split into an uplink and a downlink channels [16]. Hereinafter, the uplinks and downlinks are referred to as links or channels. Thus, the network is represented by a directed graph $\mathcal{G}(\mathcal{N}, \mathcal{L})$, in which, $\mathcal{N} = \{i : i = 1, 2, ..., n\}$ is a set of n UAV nodes and $\mathcal{L}$ is a set of l directed links, i.e., $\mathcal{L} = \{L_{i,j} : i, j \in \mathcal{N}\}$, where $L_{i,j}$ is the channel from UAV node i to UAV node j. In our model, each link has a capacity $C_{i,j}$ packets per second (pps). $C_{i,j}$ is initialized based on maximum link capacity (for example, the maximum connection capacity can be split equally between the uplink and the downlink). This initial capacity will be updated iteratively until convergence is achieved, as detailed in Subsection II-E.

We assume there is a set $\mathcal{F}$ of f traffic streams. Each stream enters the UAV network at a given node $s_k \in \mathcal{N}$ and exits at another node $d_k \in \mathcal{N}$, $k \in \{1, 2, ..., f\}$ is the flow label. Each stream has a rate of R_k pps. These rates are assumed to be constant over the route update interval. When a significant change takes place in these rates, the OLBR must re-optimize the routing parameters.

B. The Node Model

To build a mathematical optimization model for this network, we represent the UAV node as depicted in Fig. 3. As a relaying node, the UAV receives traffic flows at different

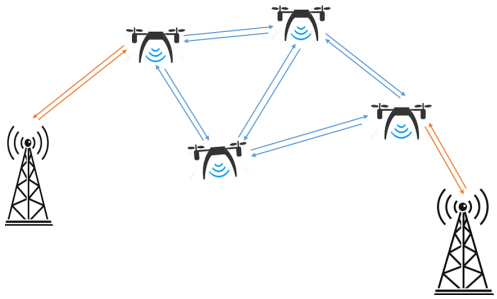

Figure 2. Network model.

Authorized licensed use limited to: Queen's University. Downloaded on December 01,2021 at 20:31:36 UTC from IEEE Xplore. Restrictions apply.

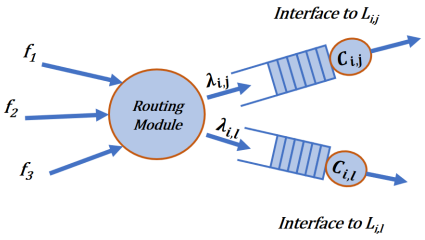

Figure 3. Node model.

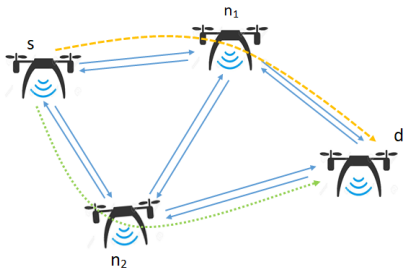

Figure 4. Node forwarding and traffic splitting.

input interfaces of download channels. These packets are processed by the routing module and each packet is forwarded to the outgoing interface of the appropriate upload channel. To achieve load-balancing, packets from the same traffic stream k may be forwarded through different interfaces. For example, in Fig. 4, there is a flow (whose label is k) from node s to node d, the source node s forwards a portion $\alpha_k^{s,1}$ of these packets to n_1 (yellow traffic) and the remainder portion ($\alpha_k^{s,2} = 1 - \alpha_k^{s,1}$) of the packets to n_2. UAV nodes n_1 and n_2 can make similar decisions. We call these portions ($\alpha_k^{i,j} \in [0,1]$) the Link-Flow Assignment (LFA) parameters which represent the portion of the k_{th} flow packets that should be routed through the link $L_{i,j}$. Therefore, the total traffic rate $\lambda_{i,j}$ that will be forwarded through each link $L_{i,j}$ is the summation of all flow portions that are forwarded through it, as represented by (1).

$$\lambda_{i,j} = \sum_k \alpha_k^{i,j} R_k \quad \text{where } \alpha_k^{i,j} \in [0,1]. \tag{1}$$

Figure 3 shows the queuing process. At the outgoing interface, packets may be queued because of the limited link capacity. We model this queueing process using the M/M/1/K queuing model [14], as shown in Fig. 3, where, the uplink interface is represented by a queue. The processing rate $C_{i,j}$ is the channel capacity in *pps*, and $\lambda_{i,j}$ is its total packet arrival rate that should be transmitted over this link. Based on this queuing model, the average delay (queuing delay + processing delay) $T_{i,j}$ that a packet experiences at a given interface $L_{i,j}$, can be computed as:

$$T_{i,j} = \frac{1}{C_{i,j} - \lambda_{i,j}}, \tag{2}$$

where $\lambda_{i,j} < C_{i,j}$. This condition is necessary to avoid dropping packets by the queue, and it will be enforced by the constraints as shown later.

C. The Routing Optimization Problem

The primary purpose of OLBR is to utilize the alternative routes by balancing packet load (belonging to the same stream) across multiple routes in such a way that minimizes the total network-wide queuing delay. So, the OLBR should compute the optimal LFA parameters, $\alpha_k^{i,j}$, for each traffic flow k.

1) The Objective Function: The objective of the OLBR is to minimize the network-wide delay. Based on (2), the total delay T_i, per time unit, at a given node i is the summation of the delays experienced at all its exit interfaces, i.e.,

$$T_i = \sum_{L_{i,j} \in \mathcal{L}} \lambda_{i,j} T_{i,j} = \sum_{L_{i,j} \in \mathcal{L}} \frac{\lambda_{i,j}}{C_{i,j} - \lambda_{i,j}}, \tag{3}$$

and the network-wide delay per time unit is the summation of T_i over all nodes, i.e.,

$$T = \sum_{i \in \mathcal{N}} T_i = \sum_{i \in \mathcal{N}} \sum_{L_{i,j} \in L} \frac{\sum_k \alpha_k^{i,j} R_k}{C_{i,j} - \sum_k \alpha_k^{i,j} R_k}. \tag{4}$$

2) The Optimization Constraints: The constraints are built to satisfy the route continuity condition, which means that any packet should be routed through a continuous route from its source to the destination. This condition can be achieved by enforcing the individual flow balance at each routing node, i.e., any intermediate relaying node forwards all the packets it receives if it is not the source or the destination of this traffic flow. Mathematically, the traffic flow balance for a flow k at an intermediate node i is formulated as:

$$\sum_{L_{i,d} \in \mathcal{L}} \alpha_k^{i,d} - \sum_{L_{s,i} \in \mathcal{L}} \alpha_k^{s,i} = 0. \tag{5}$$

In (5), the R_k should be multiplied by both terms. It is canceled because the right-hand side is zero. For the source (or the destination) of the k^{th} packet stream, the total packets that the node sends (or receives) equals to the k^{th} flow traffic rate, i.e.,

$$\begin{aligned} &\sum_{L_{i,d} \in \mathcal{L}} \alpha_k^{i,d} - 1 = 0, \qquad \text{if } i \text{ is the } k^{th} \text{ flow source ,} \\ &1 - \sum_{L_{s,i} \in \mathcal{L}} \alpha_k^{s,i} = 0, \quad \text{if } i \text{ is the } k^{th} \text{ flow destination.} \end{aligned} \tag{6}$$

These three constraints guarantee that each packet will be forwarded through a continuous route from its source to its destination.

In addition to the route continuity, another constraint is used to avoid dropping packets by the limited-size M/M/1/K queue. This constraint limits the total traffic load on any link to its capacity, i.e., $\lambda_{i,j} < C_{i,j}$, which can be written as a linear function in $\alpha_k^{i,j}$ as:

$$\sum_{k=1}^{f} \alpha_k^{i,j} R_k \leqslant C_{i,j} \quad \forall \ L_{i,j} \in \mathcal{L}. \tag{7}$$

Authorized licensed use limited to: Queen's University. Downloaded on December 01,2021 at 20:31:36 UTC from IEEE Xplore. Restrictions apply.

Finally, the last constraint is to make sure that the $\alpha_k^{i,j}$ is non-negative. The complete optimization problem is compiled in (8).

$$
\begin{aligned}
&\underset{\alpha_k^{i,j}}{\textit{minimize}}\ T = \sum_{L_{i,j}\in L} \frac{\sum_k \alpha_k^{i,j} R_k}{C_{i,j} - \sum_k \alpha_k^{i,j} R_k} \\
&\text{subject to:} \\
&\sum_{L_{i,d}\in\mathcal{L}} \alpha_k^{i,d} - \sum_{L_{s,i}\in\mathcal{L}} \alpha_k^{s,i} = 0, \quad \text{if } i \text{ is relaying the } k^{th} \text{ flow} \\
&\sum_{L_{i,d}\in\mathcal{L}} \alpha_k^{i,d} - 1 = 0, \qquad \text{if } i \text{ is the } k^{th} \text{ flow source} \\
&1 - \sum_{L_{s,i}\in\mathcal{L}} \alpha_k^{s,i} = 0, \quad \text{if } i \text{ is the } k^{th} \text{ flow destination} \\
&\sum_{k=1}^{f} \alpha_k^{i,j} R_k \leqslant C_{i,j} \quad \forall\ L_{i,j} \in \mathcal{L}, \\
&0 \leq \alpha_k^{i,j} \leq 1.
\end{aligned}
\tag{8}
$$

D. Non-linear to Linear Problem

We can see that all the constraints are linear functions of the arguments $\alpha_k^{i,j}$, but the objective is not. By analyzing the objective function, we realize that it is a summation of a set of terms. Each term is convex and monotonically increasing in the decision variable space $\alpha_k^{i,j}$ (each term can be represented as $\frac{X}{C-X}$, which is a convex function in X). And since $\alpha_k^{i,j}$ is bounded, we can solve this problem iteratively until the solution converges to its global optimum. To solve it, we assume initial value for the link delay $\widehat{T}_{i,j}$. Subsequently, the objective is formulated (based on (3) and (4)) as a linear objective function as:

$$
T = \sum_{i\in\mathcal{N}} T_i = \sum_{i\in\mathcal{N}} \sum_{L_{i,j}\in L} \lambda_{i,j} \widehat{T}_{i,j} = \sum_{i\in\mathcal{N}} \sum_{L_{i,j}\in L} \widehat{T}_{i,j} \sum_k \alpha_k^{i,j} R_k \tag{9}
$$

Using this linear objective function, and given the linear constraints, the problem can be solved using a linear programming solver. Subsequently, the $\widehat{T}_{i,j}$ is updated based on the current best estimate of the solution, using (2). This process is performed iteratively until convergence is achieved.

E. Determining the Slot Format and Updating Capacity

Since all the symbols use the same numerology, they are of equal capacities and the same coding scheme. Based on that, we can select the slot format that copes with the ratio between the uplink and the downlink traffic loads. For example, if $\lambda_{i,j}$:$\lambda_{j,i}$= 1:3, then SFI = 33 (shown in Fig. 1) is the best format since it gives 3:9 ratio between the uplink and downlink traffic loads.

Once the slot formats are selected, the link capacities can be updated. And, iteratively, the updated problem is solved until a whole system converges. The convergence here can be either by reaching a fixed SFI, which will stop the computation, or by oscillating between two or more SFIs. The oscillation may happen because the slot format itself is not continuous and may not exactly fit the traffic loads' ratios. In this case, the computation is terminated, and we select the SFI that gives the lowest delay.

F. Packet Routing

Once the optimization problem is solved, the LFA parameters can be used to stochastically forward packets. In the proposed OLBR, instead of using the destination IP address for packet routing, the routing table stores the traffic flow labels, and instead of the cost of the interface, it stores a probability $p_k^{i,j}$ for each interface, which is the probability to use this interface as the next hop for a given traffic flow label k. To compute $p_k^{i,j}$ for the k^{th} flow, the routing module in node i finds all its exit links whose $\alpha_k^{i,j} > 0$. Denoting this set of links $\widehat{\mathcal{L}}$, the routing module computes $p_k^{i,j}$ by normalizing the LFA parameters for these links, as:

$$
p_k^{i,j} = \frac{\alpha_k^{i,j}}{\sum\limits_{L_{i,j}\in\widehat{\mathcal{L}}} \alpha_k^{i,j}}. \tag{10}
$$

Subsequently, when the routing module receives a packet, it finds its flow label, k, and finds the pre-computed $p_k^{i,j}$ values for this flow. Then, from the interfaces with non-zero $p_k^{i,j}$, it stochastically selects one of these links to forward the packet.

G. Routing Loops

The proposed OLBR is a loop-free technique. The combination of the objective function and the constraints guarantees that the resulting LFA produces loop-free routes. We prove this by contradiction and show it using the example network in Fig. 4. A routing loop means that a packet can go through a given node more than once. Based on this, if an optimal routing solution has a routing loop, packets will pass the same node at least twice, which adds more queuing delay, which increases the queuing delay. This contradicts with the routing optimality that is guaranteed by the objective function.

We give a simple network example in Fig. 4. For the flow from s to d, a loop may take place if both $\alpha_k^{1,2} > 0$ and $\alpha_k^{2,1} > 0$. Based on this assignment, packets can go back to node 1 or node 2, causing a loop. If this is the optimal solution, these values for $\alpha_k^{i,j}$ also mean that, in the optimal traffic assignment, there are packets that should take the route [s, 1, 2, 1, d] (instead of [s, 1, d]) and, simultaneously, other packets take the route [s, 2, 1, 2, d] (instead of [s, 2, d]). This route assignment increases the packet queuing (compared to the [s, 1, d] and [s, 2, d] routes), which contradicts the optimal objective. Thus, in the optimal solution, $\alpha_k^{1,2}$ and $\alpha_k^{2,1}$ can't both be non-zero. This proof can be easily extended to more complex networks.

III. Simulation Results

To evaluate the proposed OLBR, we use Monte Carlo simulation to address the uncertainty in the traffic demand randomness and distribution across the network. We use two

Authorized licensed use limited to: Queen's University. Downloaded on December 01,2021 at 20:31:36 UTC from IEEE Xplore. Restrictions apply.

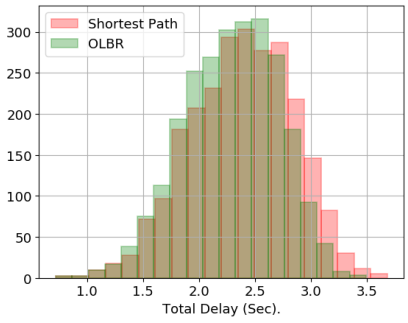

(a) Average flow rate = 800 *pps*

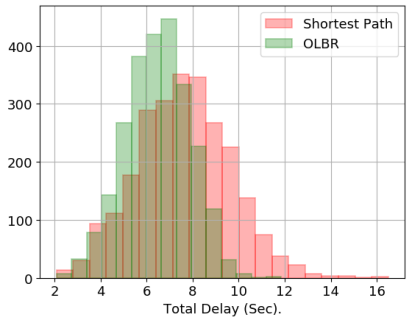

(b) Average flow rate = 1600 *pps*

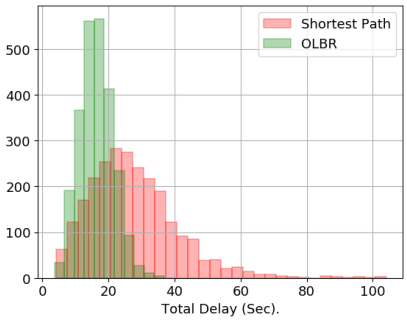

(c) Average flow rate = 2400 *pps*

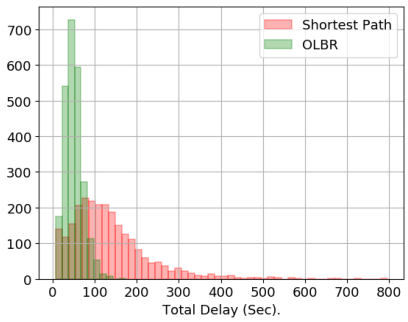

(d) Average flow rate = 3000 *pps*

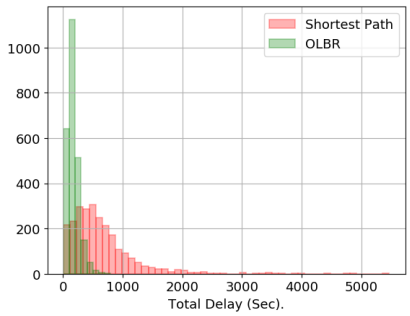

(e) Average flow rate = 4000 *pps*

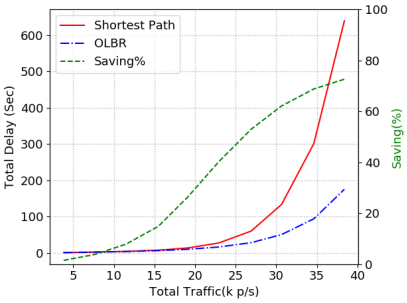

(f) Summary

Figure 5. Figures a though e the distribution of the network total delay for different traffic loads for the small network, and f is average Daley and saving.

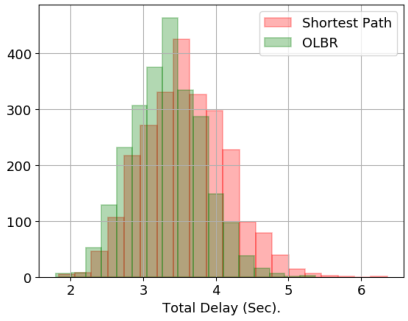

(a) Average flow rate = 1000 *pps*

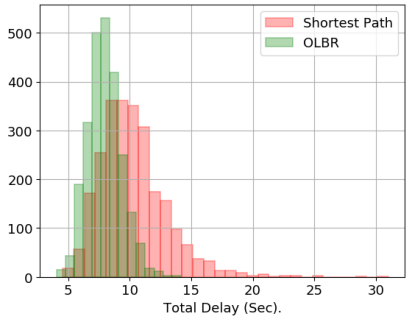

(b) Average flow rate = 2000 *pps*

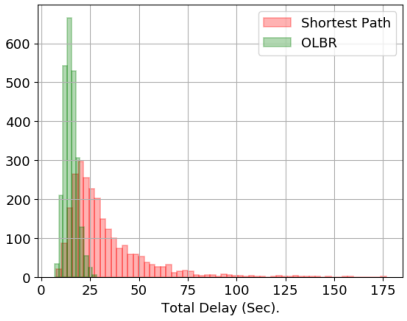

(c) Average flow rate = 3000 *pps*

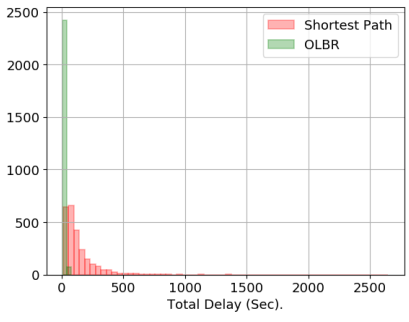

(d) Average flow rate = 4000 *pps*

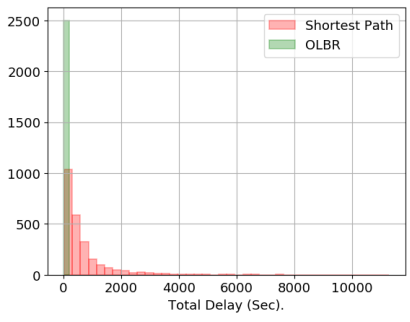

(e) Average flow rate = 5000 *pps*

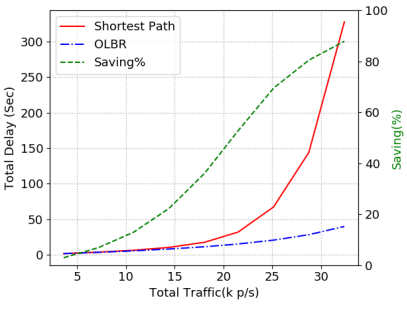

(f) Summary

Figure 6. Figures a though e the distribution of the network total delay for different traffic loads for the big network, and f is average Daley and saving.

network typologies, a small topology similar to Fig. 4 and a bigger grid topology with 9 nodes. In both networks, each link has an uplink and downlink channels, and each has a capacity of 5000 *pps*.

We use 10 different traffic levels with different average traffic flow rates. The minimum average traffic flow rate is 500 and 400 *pps* for the big and small networks, respectively. This base rate is multiplied by factors 2 through 10 to generate

Authorized licensed use limited to: Queen's University. Downloaded on December 01,2021 at 20:31:36 UTC from IEEE Xplore. Restrictions apply.

higher average rates. To address the uncertainty of the traffic loads and their distribution across the network, we generate 2500 different random traffic scenarios for each traffic level. In each of these scenarios, traffic flows are randomly generated between nodes. A traffic flow is created from node i to node j with a probability of 0.5 and 0.8 for the big network and the small network, respectively. The rates of these flows are extracted from a normal distribution centered at the average rate of this traffic level, with a coefficient of variation of 0.5. For each of these traffic scenarios, we run the OLBR and the shortest path routing. The network-wide total packet delay per time unit is computed as a comparison metric.

The simulation results are shown in Fig. 5 and 6 which compare the OLBR to the shortest path based routing. The two figures show that the OLBR improves the network performance in both a small typology and a more complex bigger typology. The figures show that, at low traffic rates, the total delay in both cases is similar. The reason is that, at low traffic demands, there is no congestion in the network and both the OLBR and the shortest path use similar routes, so the OLBR has no significant impact as shown in Fig. 5a and Fig. 6a. The subsequent figures show that as the traffic rate increases, the difference between the OLBR and the shortest path becomes significant, as shown by the delay distributions, which clarify two important differences. Firstly, the mean value (over the 2500 random scenarios) for the delay in the shortest path cases becomes significantly longer than that for the OLBR as the traffic increases. Secondly, the variance of the delay in the OLBR routing is limited compared to the shortest path. These two improvements achieved by the OLBR illustrate the importance of optimized load-balancing, especially in the case of high traffic loads.

Fig. 5f and Fig. 6f show the total network-wide packet delay per time unit in both network typologies. The figures show that the OLBR can save up to 80% of the packet delay due to the optimized load-balancing.

IV. Conclusion

In this paper, we propose a mathematical model to optimize routing performance in UAV-assisted 5G cellular networks by jointly computing the uplink and downlink capacities for each connection on one side and the optimum load-balancing traffic assignment on the other side. The proposed routing technique minimizes the network-wide delay by routing packets through multiple alternative routes simultaneously. This way, the traffic load on the shortest paths is reduced, resulting in lower queuing delay. The simulation results on various network configurations that consider the traffic load variability show that the proposed OLBR routing technique outperforms the shortest path based routing. This work is considered a first step towards routing optimization in UAV. There are many directions to extend this paper. Comparing the proposed system to other routing techniques such as genetic algorithms or reinforcement learning based routing is one important direction. Another area for further research is to utilize other objective functions such as minimizing the packet drops or energy consumption. Additionally. Also, studying the impact of load-balancing on the quality of services, especially for sensitive applications, should be considered.

References

[1] S. Chowdhury, A. Emelogu, M. Marufuzzaman, S. G. Nurre, and L. Bian, "Drones for disaster response and relief operations: A continuous approximation model," *International Journal of Production Economics*, vol. 188, pp. 167 – 184, 2017. [Online]. Available: http://www.sciencedirect.com/science/article/pii/S0925527317301172

[2] R. Lee, J. Manner, J. Kim, B. Hurley, P. Amodio, and K. Anderson, "Role of deployable aerial communications architecture in emergency communications and recommended next steps," *Federal Communications Commission*, 2011.

[3] T. Kopfstedt, M. Mukai, M. Fujita, and C. Ament, "Control of formations of uavs for surveillance and reconnaissance missions," *IFAC Proceedings Volumes*, vol. 41, no. 2, pp. 5161 – 5166, 2008, 17th IFAC World Congress. [Online]. Available: http://www.sciencedirect.com/science/article/pii/S1474667016397622

[4] R. R. Pitre, X. R. Li, and R. Delbalzo, "Uav route planning for joint search and track missions—an information-value approach," *IEEE Transactions on Aerospace and Electronic Systems*, vol. 48, no. 3, pp. 2551–2565, JULY 2012.

[5] C. Barrado, R. Messeguer, J. Lopez, E. Pastor, E. Santamaria, and P. Royo, "Wildfire monitoring using a mixed air-ground mobile network," *IEEE Pervasive Computing*, vol. 9, no. 4, pp. 24–32, October 2010.

[6] C. Eschmann, C.-M. Kuo, C.-H. Kuo, and C. Boller, "High-resolution multisensor infrastructure inspection with unmanned aircraft systems," *ISPRS-International Archives of the Photogrammetry, Remote Sensing and Spatial Information Sciences*, no. 2, pp. 125–129, 2013.

[7] L. Reynaud, T. Rasheed, and S. Kandeepan, "An integrated aerial telecommunications network that supports emergency traffic," in *2011 The 14th International Symposium on Wireless Personal Multimedia Communications (WPMC)*. IEEE, 2011, pp. 1–5.

[8] A. Guillen-Perez and M.-D. Cano, "Flying ad hoc networks: A new domain for network communications," *Sensors*, vol. 18, no. 10, p. 3571, 2018.

[9] International Business Times. (2016) Nokia and EE trial mobile base stations floating on drones to revolutionise rural 4G coverage. [Online]. Available: https://www.ibtimes.co.uk/nokia-ee-trial-mobile-base-stations-floating-drones-revolutionise-rural-4g-coverage-1575795

[10] 3GPP, "Physical channels and modulation," 3rd Generation Partnership Project (3GPP), Technical Specification (TS), 06 2020, v16.0.0.

[11] 3GPP, "Physical layer procedures for control," 3rd Generation Partnership Project (3GPP), Technical Specification (TS), 10 2018, v16.0.0.

[12] M. Polese, M. Giordani, T. Zugno, A. Roy, S. Goyal, D. Castor, and M. Zorzi, "Integrated access and backhaul in 5G mmwave networks: Potential and challenges," *IEEE Communications Magazine*, vol. 58, no. 3, pp. 62–68, 2020.

[13] K. Singh and A. K. Verma, "Applying olsr routing in fanets," in *2014 IEEE International Conference on Advanced Communications, Control and Computing Technologies*, 2014, pp. 1212–1215.

[14] L. Kleinrock, *Queuing Systems, Volume 2: Computer Applications*. wiley New York, 1976, vol. 66.

[15] S. Amante, B. Carpenter, S. Jiang, and J. Rajahalme, "IPv6 Flow Label Specification," Internet Requests for Comments, IETF, RFC 6437, November 2011. [Online]. Available: https://www.rfc-editor.org/rfc/rfc6437.txt

[16] Y. Zeng, Q. Wu, and R. Zhang, "Accessing from the sky: A tutorial on uav communications for 5G and beyond," *Proceedings of the IEEE*, vol. 107, no. 12, pp. 2327–2375, Dec 2019.

Authorized licensed use limited to: Queen's University. Downloaded on December 01,2021 at 20:31:36 UTC from IEEE Xplore. Restrictions apply.